

Orthorhombic and monoclinic ferroelectric phases investigated by Raman spectroscopy in PZN-4.5%PT and PZN-9%PT crystals

Mimoun El Marssi^{a,*}, Hichem Dammak^b

^aLaboratoire de Physique de la Matière Condensée, Université de Picardie Jules Verne, 33 rue Saint-Leu 80039 Amiens Cedex, France

^bLaboratoire Structure Propriétés et Modélisation des Solides, UMR 8580, Ecole Centrale Paris, Grande Voie des Vignes, 92295 Châtenay-Malabry Cedex, France

Received 5 March 2007; received in revised form 30 March 2007; accepted 11 April 2007 by E.V. Sampathkumaran

Available online 19 April 2007

Abstract

Polarized Raman spectra measurements have been performed on orientated single crystals of $\text{Pb}[(\text{Zn}_{1/3}\text{Nb}_{2/3})_{0.955}\text{Ti}_{0.045}]_3\text{O}_3$ (PZN-4.5%PT) and $\text{Pb}[(\text{Zn}_{1/3}\text{Nb}_{2/3})_{0.91}\text{Ti}_{0.09}]_3\text{O}_3$ (PZN-9%PT) poled by an electric field along the $[\bar{1}01]$ pseudo-cubic direction in order to determine the nature of the induced ferroelectric phases. Under field-cooled (FC) conditions the ferroelectric phase transition sequence, tetragonal–orthorhombic–rhombohedral, was observed in PZN-4.5%PT. Comparison between the phase transitions induced in PZN-9%PT and PZN-4.5%PT crystals in FC shows that the low-temperature ferroelectric phase in PZN-9%PT cannot be orthorhombic and it can be attributed to the monoclinic phase. The characteristic temperatures found by Raman spectroscopy correspond to those obtained by dielectric measurements and by X-ray diffraction reported previously.

© 2007 Elsevier Ltd. All rights reserved.

PACS: 77.84.Dy; 78.30.-j

Keywords: A. Ferroelectrics; C. Crystal structure and symmetry; D. Phase transitions; E. Raman spectroscopy

1. Introduction

Relaxor-based ferroelectric materials such as $\text{Pb}[(\text{Mg}_{1/3}\text{Nb}_{2/3})_{1-x}\text{Ti}_x]_3\text{O}_3$ (PMN- x %PT) and $\text{Pb}[(\text{Zn}_{1/3}\text{Nb}_{2/3})_{1-x}\text{Ti}_x]_3\text{O}_3$ (PZN- x %PT) have attracted a lot of interest in the last decade because of their substantial piezoelectric and electromechanical properties. These properties are especially enhanced near the morphotropic phase boundary (MPB) that separates the rhombohedral (R) and the tetragonal (T) phases. Such behaviour is a common feature of the well-known $\text{Pb}(\text{Zr}_x\text{Ti}_{1-x})_3\text{O}_3$ (PZT) systems. This region is located approximately at 35% of PT for PMN-PT [1] and at 9% of PT for PZN-PT [2]. The exceptional electromechanical properties of PZT, PMN-PT, and PZN-PT have recently been attributed to the polarization rotation mechanism in the intermediate monoclinic (called M_A , M_B or M_C : see [3] for significations) phase occurring close to the MPB [4–8]. The

transition sequence $R-M_B-O-M_C-T$ predicted by Vanderbilt and Cohen [3] is well evidenced [9,10] in PMN-PT but continues to be debated in PZN-PT. Studies by X-ray and neutron diffraction have shown that the low temperature phase for PZN-PT around the MPB composition should be monoclinic (M_C) with space group Pm [11–14]. In previous works, this low temperature phase has been attributed to the orthorhombic phase (O) [2,15]. In addition, it was shown to be possible to obtain a stable quasi-single monoclinic (M_C) domain state by poling a PZN-9%PT single crystal along the pseudo-cubic $[\bar{1}01]$ direction [11,16]. (In all the paper crystallographic directions and planes were indexed using the pseudo-cubic axes of the perovskite cell.) Recently, using a micro-Brillouin scattering technique, Ko et al. [17] suggested that this induced phase can be attributed to an orthorhombic phase. At the same time, in a PZN-4.5%PT single crystal, Liu and Lynch [18] demonstrated by optical observations and hysteresis loop measurements that when an electric field larger than 11 kV/cm is applied along $[\bar{1}01]$ direction, a rhombohedral to orthorhombic phase transition takes place at room temperature. Renault et al. [19] demonstrated by

* Corresponding author.

E-mail address: mimoun.elmarssi@u-picardie.fr (M. El Marssi).

X-ray diffraction that the O phase with C_{2v} symmetry in PZN-4.5%PT can also be induced under field-cooled (FC) conditions between the R and T phases in the 365–390 K temperature range.

The characterization of the phase symmetry of these compounds by Raman scattering is known to be complicated [20–26]. For example, Raman scattering bands were observed in the paraelectric phase having an average cubic ($Pm\bar{3}m$) symmetry where Raman activity is forbidden, and in going from the paraelectric to the ferroelectric phase, no narrowing of the Raman lines was observed. This behaviour was attributed to the translational symmetry breaking induced by the chemical disorder on the B site and to atomic displacement disorder as confirmed recently by lattice dynamics calculations and spectra simulations [27].

In spite of the complexity of the scattering processes in relaxors and relaxor-based ferroelectrics and of the difficulties of mode assignment in the ferroelectric phase [28], it has been shown that the temperature variation of the Raman spectra and the intensity of some modes can be associated with the structural phase transitions [20,23,25,26,29].

Up to now, most of the Raman studies reported on PZN-PT and PMN-PT were made on crystals oriented and/or poled along the [001] pseudo-cubic axes [20–23], which is not the appropriate direction to characterize rhombohedral, orthorhombic or the monoclinic ferroelectric phases. In addition, multi-domain states were obtained after poling along this direction. In the present work, we report for the first time polarized Raman spectra of single crystals of PZN-4.5%PT and PZN-9%PT poled by an electric field along the $[\bar{1}01]$ direction. The purpose is to compare the Raman scattering behaviour of the induced orthorhombic single domain state in PZN-4.5%PT and the monoclinic quasi-single domain state of PZN-9%PT. Since we cannot attribute any phase symmetry using the zone-centre mode assignment, we compare in FC the T – M phase transition in PZN-9%PT and the T – O phase transition in PZN-4.5%PT and demonstrate that these transitions are different. Contrary to what was reported previously [17] we show that the low-temperature phase in PZN-9%PT crystal can be monoclinic.

2. Experiment

The single crystals PZN-4.5%PT and PZN-9%PT were grown by the flux method [11]. They were orientated and cut with the faces perpendicular to the orthorhombic axes using the Laüé technique. The samples have parallelepiped shape with sizes $1.9 \times 1.4 \times 1.3 \text{ mm}^3$ for PZN-4.5%PT crystal and $1.7 \times 1.2 \times 0.7 \text{ mm}^3$ for PZN-9%PT crystal. The large faces of both the crystals are perpendicular to the [101] (X -direction) and the smaller faces are perpendicular to [010] (Y -direction) and to $[\bar{1}01]$ (Z -direction). Both samples showed high optical quality to the light scattering studies. A semitransparent gold layer was sputtered on to the $(\bar{1}01)$ faces. The electrical contact between gold wires and thin film electrodes was ensured by gold paste. The domain pattern can be observed between crossed polarizers. The light was transmitted through the sample along

the $[\bar{1}01]$ direction. The Raman signals were taken through the gold electrodes.

Raman measurements were performed in a backscattering microconfiguration, using the 514.5 nm light from an argon ion laser focused on the sample surface as a spot of 2 μm in diameter. The scattered light was dispersed by a subtractive triple Jobin Yvon spectrometer (Model T64000) and collected with a liquid nitrogen cooled CCD detector. The spectrometer had a wave number resolution better than 3 cm^{-1} . All the spectra have been corrected for the Bose–Einstein factor. The external electric field was applied in $[\bar{1}01]$ direction (Z) and the temperature is controlled by using a Linkam TS 600 hot stage with a temperature stability of $\pm 0.1 \text{ K}$. Raman spectra were recorded during FC conditions with $E = 1 \text{ kV/cm}$. The dielectric susceptibility measurements under FC conditions were carried out prior to the Raman measurements in order to determine the phase-transition temperatures. Electrical impedance of the samples was measured using a HP 9194 impedance analyser at 1 kHz and with a cooling constant rate of 2 K/min.

3. Results and discussion

When an E-field is applied along an off-polar direction of a crystal, it leads to the setting up of a multidomain configuration which depends on the E-field direction. The domain configurations of the R , T and O phases were described in previous papers [11,19,30]. For the E-field direction $[\bar{1}01]$, they were designated as $2R$, $2T$, and $1O$. The digit stands for the number of equivalent ferroelectric domains. The monoclinic phase for which the polar direction makes an angle of a few degrees with the poling $[\bar{1}01]$ direction leads to a quasi-single domain that we call 1M.

Fig. 1 shows that for PZN-9%PT, the cubic–tetragonal ($C \rightarrow 2T$) phase-transition occurs at 450 K and the low temperature phase transition tetragonal–monoclinic ($2T \rightarrow 1M$) occurs at 300 K. For PZN-4.5%PT we observe three phase transitions $C \rightarrow 2T \rightarrow 1O \rightarrow 2R$ at 430, 390, and 360 K. In the following we are interested in the ferroelectric transitions starting from the $2T$ state which is the same in both PZN-4.5%PT and PZN-9%PT crystals.

Parallel $Z(XX)\bar{Z}$ and crossed $Z(XY)\bar{Z}$ Raman spectra recorded under FC conditions at several temperatures for PZN-4.5%PT and for PZN-9%PT are plotted in Figs. 2 and 3. In the tetragonal phase, the spectra of the two crystals seem very similar: all lines are of the same shape and are located at the same frequencies. However, small differences do exist between the spectra of the tetragonal phase for the two crystals. For instance, the 780 cm^{-1} mode in crossed spectra (Fig. 3) is more intense in PZN-9%PT. This difference can be attributed to the higher PT concentration and to the fact that the crystal exhibits the $2T$ multidomain state. It has been shown that ratio of band intensities depends on the domain wall structure in the region where the laser beam is focused [25].

For the PZN-9%PT sample, an important change of the parallel Raman spectra is observed at the tetragonal–monoclinic transition temperature ($T_{T-M} \approx 300 \text{ K}$). Except for the high

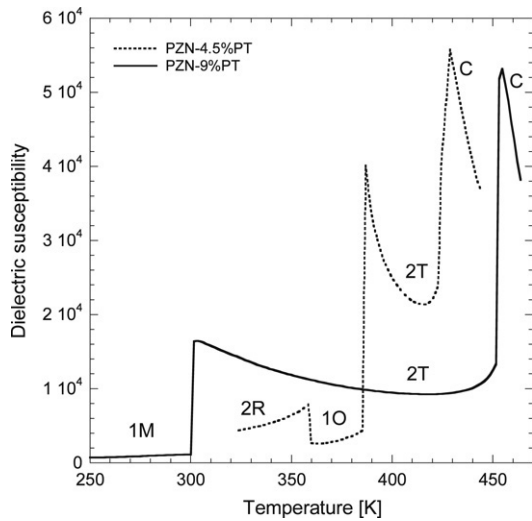


Fig. 1. Temperature dependence of the dielectric susceptibility at 1 kHz along $[101]$ of PZN-4.5%PT and PZN-9%PT crystals recorded under FC conditions. Ferroelectric phase and domain families are indicated as follows: tetragonal (2T), single orthorhombic domain (1O), rhombohedral (2R) and quasi-single monoclinic domain (1M).

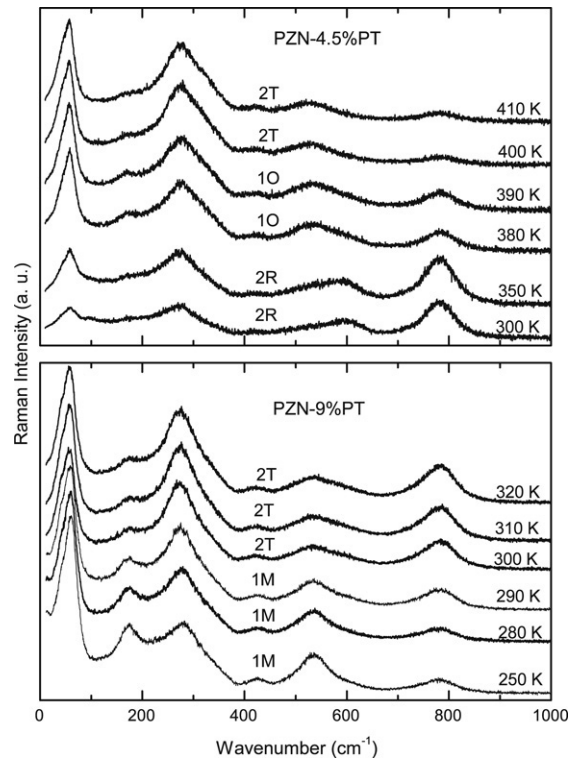


Fig. 3. Temperature dependence of the crossed Raman spectra $Z(XY)\bar{Z}$ of PZN-4.5%PT and PZN-9%PT crystals recorded under FC conditions in tetragonal (2T), orthorhombic (1O), rhombohedral (2R) and monoclinic (1M) phases.

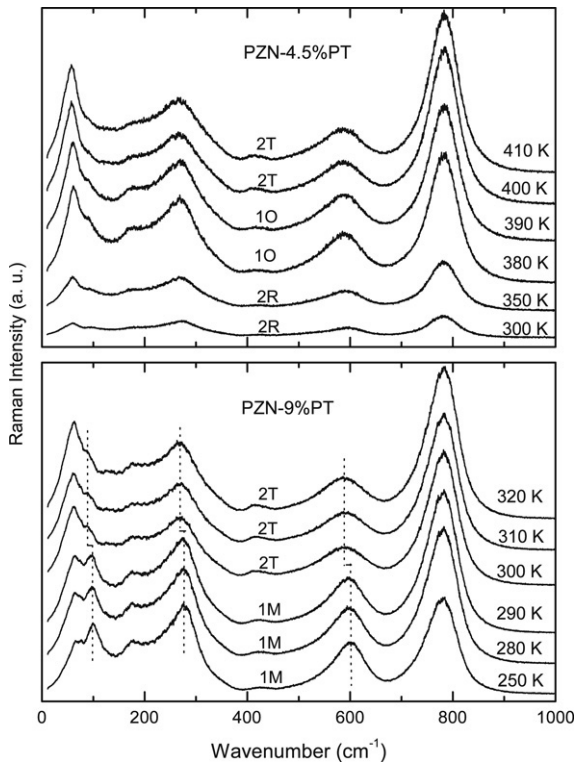


Fig. 2. Temperature dependence of the parallel Raman spectra $Z(XX)\bar{Z}$ of PZN-4.5%PT and PZN-9%PT crystals recorded under FC conditions in tetragonal (2T), orthorhombic (1O), rhombohedral (2R) and monoclinic (1M) phases.

frequency mode, the width of all Raman lines decreases and a shift to high frequency of some modes is observed (Fig. 2). In contrast, only small changes are observed in the case of PZN-4.5%PT at the tetragonal–orthorhombic temperature transition ($T_{T-O} \approx 390$ K).

Fig. 4, shows the temperature variation of frequency for some modes in PZN-4.5%PT and PZN-9%PT crystals near the transition temperatures T_{T-O} and T_{T-M} . For PZN-4.5%PT, only a weak increase of the frequency of the low frequency mode is observed in the orthorhombic phase, while in the PZN-9%PT crystal the frequencies of the four modes increase abruptly in the monoclinic phase. In addition, for this latter phase the intensity of the low frequency mode decreases while the intensity of the mode located at 96 cm^{-1} increases. The integrated Raman intensity of this mode ($I_{96\text{ cm}^{-1}}$) was determined at each temperature using a fitting-deconvolution procedure. Fig. 5 shows the temperature dependence of the intensity ratio $I_{96\text{ cm}^{-1}}/I_T$, where I_T is the integrated intensity of the total parallel spectrum. We observe an abrupt increase of the integrated intensity of this mode at the $T-M$ transition. At lower temperatures this intensity remains constant.

The phase transitions are also observed in the crossed $Z(XY)\bar{Z}$ Raman spectra (Fig. 3). For PZN-9%PT, at $T = T_{T-M}$ the intensity of lines at 60 , 173 , and 536 cm^{-1} increases in the monoclinic phase, while the intensity of the 280 and 780 cm^{-1} lines decreases. In PZN-4.5%PT the intensity of the high frequency mode increases below $T = T_{T-O}$ while it decreases in parallel geometry. This behaviour is accentuated in the rhombohedral phase. In addition the intensity of the $Z(XX)\bar{Z}$ spectrum decreases in the rhombohedral phase and both polarization geometries $Z(XX)\bar{Z}$ and $Z(XY)\bar{Z}$ exhibit quite similar spectra. As mentioned above, this is due to the fact that the crystal exhibits the multidomain state 2R and

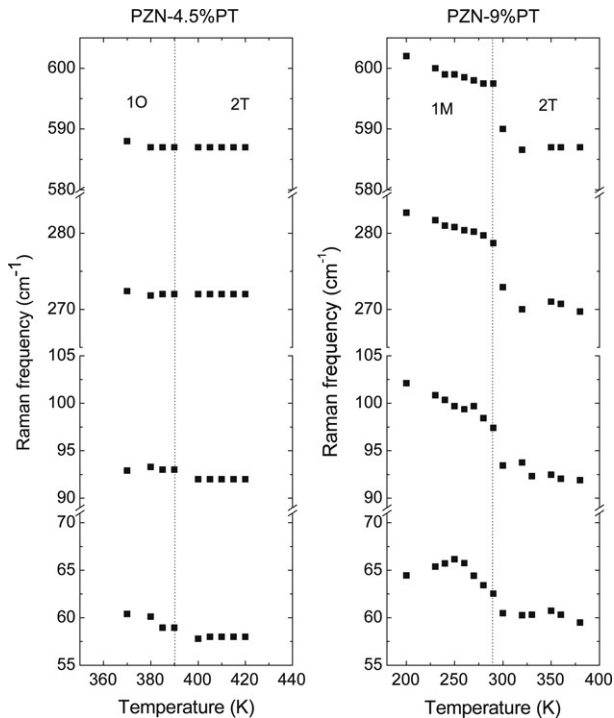


Fig. 4. Temperature evolution of some frequency modes for the tetragonal (2T), orthorhombic (1O), and monoclinic (1M) phases for PZN-4.5%PT and PZN-9%PT crystals under FC conditions.

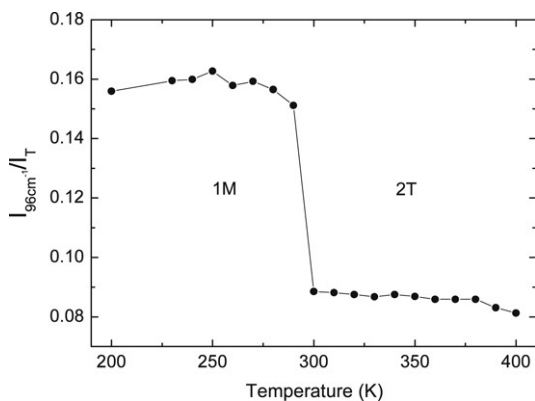


Fig. 5. Temperature dependence of the ratio of the integrated Raman intensity of the 96 cm^{-1} mode to the integrated intensity of the total parallel spectrum of PZN-9%PT crystal under FC conditions.

so depolarization of the Raman spectra occurs because the rhombohedral microdomains are optically birefringent [25,26, 28,29]. This depolarization effect is mainly described by the depolarization ratio I_{XY}/I_{XX} for the high frequency mode. It was evidenced previously that the temperature evolution of this depolarization ratio can indicate phase transitions in the relaxor-based ferroelectric materials [23,25,26]. Fig. 6 shows that in the FC process, the depolarization ratio is very weak in the tetragonal phase and increases slowly in the orthorhombic phase. In the rhombohedral phase the depolarization ratio increases more drastically and continuously when the temperature decreases to room temperature. The temperature transitions of $2T \rightarrow 1O$ and $1O \rightarrow 2R$ obtained from Raman results and from the evolution of the intensity

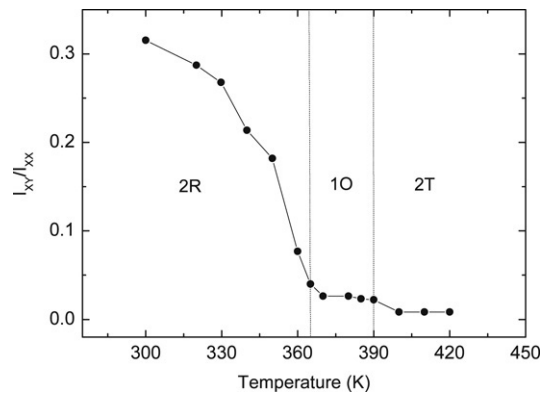


Fig. 6. Temperature evolution of the intensity ratio of the crossed to the parallel component of the 780 cm^{-1} mode of the PZN-4.5%PT crystal measured under FC conditions in tetragonal (2T), orthorhombic (1O), rhombohedral (2R) phases.

depolarization ratio in each phase are in the good agreement with dielectric measurement (Fig. 1).

The Raman results show the same characteristics in the tetragonal phase for both crystals. The low temperature phase induced in the PZN-9%PT crystal has a different response than that of the orthorhombic and the rhombohedral phases induced in PZN-4.5%PT crystal. We conclude that the low temperature phase in the PZN-9%PT crystal is not orthorhombic, and consequently it can be monoclinic.

4. Conclusions

Raman scattering was used to characterize the ferroelectric phases in poled PZN-4.5%PT and PZN-9%PT single crystals orientated along the orthorhombic axes. Since we cannot attribute any phase symmetry using the zone-centre mode assignment due to the breaking of the translation symmetry, the macrodomain ferroelectric phases in PZN-4.5%PT and PZN-9%PT crystals could not be described by the Raman mode assignment. However, a comparison of the phase transitions induced in PZN-4.5%PT and in PZN-9%PT crystals under FC conditions shows that these ferroelectric phases are different. Consequently it suggests unambiguously that the low temperature ferroelectric phase in PZN-9%PT crystal can not be orthorhombic, contrary to what has been reported previously [2,17]. In addition, polarized Raman measurements show the characteristics of the orthorhombic and the rhombohedral phases induced in PZN-4.5%PT crystal.

Acknowledgements

The authors are grateful to M. Pham Thi and A.É. Renault for crystals they have provided us and gratefully acknowledge helpful discussions with I. Lukyanchuk, M.G. Karkut and G. Calvarin. This work was partially supported by the Regional European Development Funds.

References

- [1] B. Noheda, D.E. Cox, G. Shirane, J. Gao, Z.G. Ye, Phys. Rev. B 66 (2002) 54104.

- [2] D. La-Orauttapong, B. Noheda, Z.G. Ye, P.M. Gehring, J. Toulouse, D.E. Cox, G. Shirane, Phys. Rev. B 65 (2002) 144101.
- [3] D. Vanderbilt, M.H. Cohen, Phys. Rev. B 63 (2001) 094108.
- [4] H. Fu, R.E. Cohen, Nature (London) 403 (2000) 281.
- [5] L. Bellaiche, D. Vanderbilt, Phys. Rev. Lett. 83 (1999) 1347.
- [6] B. Noheda, R. Guo, S.E. Park, D.E. Cox, G. Shirane, Phys. Rev. B 61 (2000) 8687.
- [7] B. Noheda, D.E. Cox, G. Shirane, R. Guo, B. Jones, L.E. Cross, Phys. Rev. B 63 (2000) 14103.
- [8] D.M. Hatch, H.T. Stokes, R. Ranjan, Ragini, S.K. Mishra, D. Pandey, B.J. Kenedy, Phys. Rev. B 65 (2002) 212101. And references therein.
- [9] A.K. Singh, D. Pandey, Phys. Rev. B 67 (2003) 064102.
- [10] A.K. Singh, D. Pandey, O. Zaharko, Phys. Rev. B 68 (2003) 172103.
- [11] A.É. Renault, H. Dammak, G. Calvarin, M. Pham Thi, P. Gaucher, Jpn. J. Appl. Phys. 41 (2002) 3846.
- [12] Y. Uesu, M. Matsuda, Y. Yamada, K. Fujishiro, D.E. Cox, B. Noheda, G. Shirane, J. Phys. Soc. Japan 71 (2003) 960.
- [13] R. Betram, G. Reck, R. Uecker, J. Cryst. Growth 253 (2003) 212.
- [14] J.M. Kiat, Y. Uesu, B. Dkhil, M. Matsuda, C. Malibert, G. Calvarin, Phys. Rev. B 65 (2002) 64106.
- [15] D.E. Cox, B. Noheda, G. Shirane, Y. Uesu, K. Fujishiro, Y. Yamada, Appl. Phys. Lett. 79 (2002) 400.
- [16] H. Dammak, A.É. Renault, P. Gaucher, M. Pham Thi, G. Calvarin, Jpn. J. Appl. Phys. 42 (2003) 6477.
- [17] J.H. Ko, D.H. Kim, S. Kojima, Appl. Phys. Lett. 83 (2003) 2037.
- [18] T. Liu, C.S. Lynch, Acta Mater. 51 (2003) 407.
- [19] A.É. Renault, H. Dammak, G. Calvarin, P. Gaucher, M. Pham Thi, J. Appl. Phys. 97 (2005) 044105.
- [20] F. Jiang, S. Kojima, Jpn. J. Appl. Phys. 38 (1999) 5128.
- [21] M. Iwata, H. Hoshino, H. Orihara, H. Ohwa, N. Yasuda, Y. Ishibashi, Jpn. J. Appl. Phys. 39 (2000) 5691.
- [22] H. Ohwa, M. Iwata, H. Orihara, N. Yasuda, Y. Ishibashi, J. Phys. Soc. Japan 70 (2001) 3149.
- [23] S. Kim, I.S. Yang, J.K. Lee, K.S. Hong, Phys. Rev. B 64 (2001) 94105.
- [24] O. Svitelskiy, J. Toulouse, G. Yong, Z.G. Ye, Phys. Rev. B 68 (2003) 104107. And references therein.
- [25] A. Lebon, M. El Marssi, R. Farhi, H. Dammak, G. Calvarin, J. Appl. Phys. 89 (2001) 3947.
- [26] M. El Marssi, R. Farhi, Yu.I. Yuzyuk, J. Phys.: Condens. Matter 10 (1998) 9161.
- [27] S.A. Prosandeev, E. Cockayne, B.P. Burton, S. Kamba, J. Petzelt, Yu. Yuzyuk, R.S. Katiyar, S.B. Vakhruhev, Phys. Rev. B 70 (2004) 134110.
- [28] J. Toulouse, F. Jiang, O. Svitelskiy, W. Chen, Z.G. Ye, Phys. Rev. B 72 (2005) 184106.
- [29] M. El Marssi, R. Farhi, D. Viehland, J. Appl. Phys. 81 (1997) 355.
- [30] A.É. Renault, H. Dammak, G. Calvarin, M. Pham Thi, P. Gaucher, Proceeding of the 13th IEEE, ISAF, 2002. pp. 439–442.